

BOLD MRI to evaluate early development of renal injury in a rat model of diabetes

Journal of International Medical Research
2018, Vol. 46(4) 1391–1403
© The Author(s) 2018
Reprints and permissions:
sagepub.co.uk/journalsPermissions.nav
DOI: 10.1177/0300060517743826
journals.sagepub.com/home/imr



Qidong Wang^{1,*}, Chuangen Guo^{1,*},
Lan Zhang², Rui Zhang¹, Zhaoming Wang³,
Ying Xu⁴ and Wenbo Xiao^{1,2}

Abstract

Objective: To investigate changes in renal oxygenation levels by blood-oxygenation-level dependent (BOLD)-magnetic resonance imaging (MRI), and to evaluate BOLD-MRI for detecting early diabetic renal injury.

Methods: Seventy-five rats, with unilateral nephrectomy, were randomly divided into streptozotocin-induced diabetes mellitus (DM, $n=65$) and normal control (NC, $n=10$) groups. BOLD-MRI scans were performed at baseline (both groups) and at 3, 7, 14, 21, 28, 35, 42, 49, 56, 63 and 70 days (DM only). Renal cortical (C) and medullary (M) $R2^*$ signals were measured and $R2^*$ medulla/cortex ratio (MCR) was calculated.

Results: DM-group $CR2^*$ and $MR2^*$ values were significantly higher than NC values following diabetes induction. $R2^*$ values increased gradually and peaked at day 35 ($CR2^*$, $33.95 \pm 0.34 \text{ s}^{-1}$; $MR2^*$, $43.79 \pm 1.46 \text{ s}^{-1}$), then dropped gradually ($CR2^*$, $33.17 \pm 0.69 \text{ s}^{-1}$; $MR2^*$, $41.61 \pm 0.95 \text{ s}^{-1}$ at day 70). DM-group MCR rose gradually from 1.12 to 1.32 at day 42, then decreased to 1.25 by day 70.

Conclusions: BOLD-MRI can be used to non-invasively evaluate renal hypoxia and early diabetic renal injury in diabetic rats. MCR may be adopted to reflect dynamic changes in renal hypoxia.

Keywords

Blood oxygen level dependent, magnetic resonance imaging, kidney, diabetes, renal injury

Date received: 1 May 2017; accepted: 31 October 2017

⁴Department of Nephrology, The First Affiliated Hospital, School of Medicine, Zhejiang University, Hangzhou, China

*These authors contributed equally to this work

Corresponding author:

Wenbo Xiao, The Fourth Affiliated Hospital, School of Medicine, Zhejiang University, N1 Shangcheng Road, Yiwu, 310003, China.
Email: xiaowenbo@zju.edu.cn

¹Department of Radiology, The First Affiliated Hospital, School of Medicine, Zhejiang University, Hangzhou, China
²Department of Radiology, The Fourth Affiliated Hospital, School of Medicine, Zhejiang University, Yiwu, China
³Department of Pathology, The First Affiliated Hospital, School of Medicine, Zhejiang University, Hangzhou, China



Creative Commons Non Commercial CC-BY-NC: This article is distributed under the terms of the Creative Commons Attribution-NonCommercial 4.0 License (<http://www.creativecommons.org/licenses/by-nc/4.0/>)

which permits non-commercial use, reproduction and distribution of the work without further permission provided the original work is attributed as specified on the SAGE and Open Access pages (<https://us.sagepub.com/en-us/nam/open-access-at-sage>).

Introduction

Diabetic nephropathy is a microvascular complication of diabetes mellitus and the leading cause of end-stage renal failure.¹ Renal hypoxia caused by microvascular disease, is closely related to continuous renal injury and eventually leads to diabetic nephropathy.² Functional (f) magnetic resonance imaging (MRI) is a rapidly developing imaging technology that enables the evaluation of organ function and pathology.^{3,4} Blood-oxygenation-level dependent (BOLD)-MRI, a type of fMRI, can be used to noninvasively monitor oxygen content in tissue, and to elucidate metabolic status.^{5,6} This technique is performed with the aid of an endogenous contrast agent, namely paramagnetic deoxyhaemoglobin, interfering with magnetic spin dephasing of blood water protons, which results in a BOLD enhancement effect.⁷ It has been shown that the renal R2* value is positively related to the level of deoxyhaemoglobin in tissue, while the latter is correlated with oxygen partial pressure.^{5,8}

The application of BOLD-MRI in diabetic nephropathy has been studied in animal models and in patients with diabetes.^{9–11} Use of BOLD-MRI with an animal model of diabetic nephropathy revealed that diabetic renal oxygen content was significantly decreased compared with controls.⁹ In addition, a decrease in oxyhaemoglobin was detected as early as 2 days following administration of streptozotocin (STZ) in a rat model of diabetes, and was suggestive of renal hypoxia.¹⁰ The above animal studies generally focused on selected time-points during early diabetic renal injury, and lacked dynamic and continuous observation, while clinical research has mainly concentrated on patients at later stages, as early stages are difficult to diagnose due to lack of symptoms.^{11,12} In addition, results from clinical studies may be influenced by certain drugs (such as antihypertensive drugs or

diuretics), and limited availability of renal biopsy tissue remains a problem.

Streptozotocin can accelerate pathological kidney changes in rats following unilateral nephrectomy,^{13,14} and is a preferred choice for creating an animal model of diabetes, as it selectively damages pancreatic β cells, leading to increased blood glucose, while having little effect on other organs.¹⁵

Based on the above findings, the aim of the present study was to use BOLD-MRI to track changes in renal oxygenation over time, in an STZ-induced rat model of diabetes compared with normal control rats.

Materials and methods

Animal model and study design

A total of 80 healthy male Sprague-Dawley rats (aged 4–6 weeks; weight, 150–170 g) were provided by the experimental animal centre of the First Affiliated Hospital of Zhejiang University School of Medicine, Hangzhou, China. All procedures were approved by the ethics committee on the use of animals in experimentation, namely, the Animal Experimental Ethical Inspection committee of the First Affiliated Hospital, School of Medicine, Zhejiang University, and were performed in accordance with the standards of the Chinese Association for Laboratory Animal Sciences (<http://english.calas.org.cn/>). The rats were provided with free access to water and normal diet, and housed in a well-ventilated environment maintained at 18–25°C, with a relative humidity of 40–70% and 12 h of light daily.

As the left kidney is easily affected by bowel gas, all rats in the present study underwent left kidney resection, followed by one week of enhanced care (daily or more regular bedding change, increased food and water changes). A total of 80 rats then received the normal care regime for one week, and those without weight loss during

the week were further tested for blood glucose, serum creatinine and urea nitrogen levels via tail vein samples. A total of 75 rats with normal blood glucose and renal function ranges (weight, 200–230g) were randomly divided into a nephrectomised diabetes mellitus group (DM, $n=65$) and normal control group (NC, $n=10$). The rat model of diabetes (DM group) was established by intraperitoneal injection of 65 mg/kg STZ¹⁶ (Sigma-Aldrich, St Louis, MO, USA) dissolved in 0.1 mol/l citric acid-sodium citrate buffer (pH 4.6), following a 12 h fast, and the NC group was administered an equivalent volume of 0.1 mol/l citric acid-sodium citrate buffer (pH 4.6) by intraperitoneal injection. Blood glucose from tail vein samples was measured using Contour® TS blood glucose test strips (Bayer Health Care, Leverkusen, Germany) at 3 days following injection. Fasting blood glucose levels ≥ 16.7 mmol/l were considered to indicate successful modelling. The upper limit for the test strip assay is 33.3 mmol/l, so blood glucose measurements above 33.3 mmol/l were recorded as ≥ 33.3 mmol/l.

Rats allocated to the DM group were divided into five subgroups, giving five DM groups and one NC group. During the study, one group of rats was randomly selected for MRI scanning and for 24 h urinary albumin excretion at each-time point (3, 7, 14, 21, 28, 35, 42, 49, 56, 63 and 70 days) following induction of diabetes. At day 7, 21, 35, 56 and 70, respectively, blood creatinine and urea nitrogen were also tested from tail vein samples, following the BOLD-MRI scan. These rats were then euthanized by intraperitoneal injection of 150 mg/kg pentobarbital, and the kidney was excised for histopathological examination.

MRI and data analysis

Magnetic resonance imaging measurements were acquired using a Signa HDxt 3.0T MRI scanner (GE Healthcare, Chicago,

IL, USA). The rats were anaesthetized by intraperitoneal injection with 0.007 ml/g of 4% chloral hydrate (supplied by the pharmaceutical preparation centre of the First Affiliated Hospital, School of Medicine, Zhejiang University). During imaging, animals were placed in a supine and head advanced position within an HD T/R Knee Array 8-channel phase array coil (Invivo, Gainesville, FL, USA). To reduce image artefacts caused by breathing movements, limbs were fixed by adhesive tape and the abdomen was wrapped in gauze.

The BOLD MRI T2* weighted images were acquired in coronal plane using a fast-spoiled gradient recovery sequence. MRI parameters included: repetition time, 100 ms; echo time (TE) series, 1.7 ms, 3.8 ms, 5.9 ms, 8 ms, 10.1 ms, 12.2 ms, 14.3 ms, and 16.4 ms; echo numbers, 8; flip angle, 30°; receiver bandwidth, 31.5 kHz; field of view, 60 mm \times 60 mm; slice thickness, 2.0 mm; intersection gap, 0.2 mm; acquisition matrix, 64 \times 64; and number of excitations, 2. The T2* and R2* images were obtained using Advantage workstation 4.4 (GE Healthcare), which supports FuncTool software (GE Healthcare) for automated images post-processing, and automatically generates curves for BOLD signal intensities against different TEs (Figure 1). R2* medulla to cortex ratio (MCR) was also calculated.

All Bold measurements were obtained from the processed R2* images using the region of interest (ROI) method. To avoid the influence of artefacts, ROIs should be placed as far as possible from each other and avoiding vessels visible to the naked eye. Besides artefacts, the setting of ROIs must also be considered, because a slight variation in placement, size or shape of an ROI in the rat kidney may lead to different results. Thus, the placement of ROIs on an R2* image was determined by two experienced radiologists (QW and CG) reaching a consensus through discussion. As a result,

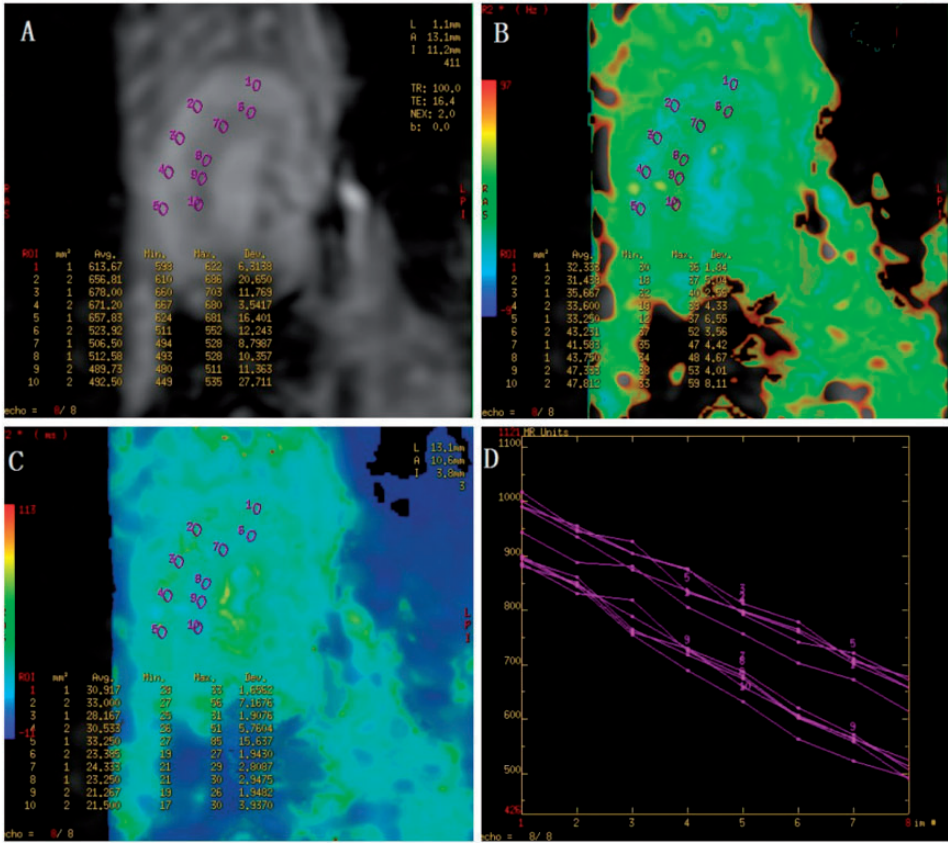


Figure 1. Representative images obtained using blood-oxygenation-level dependent (BOLD)- magnetic resonance imaging (MRI) with Advantage workstation 4.4 and FuncTool software to assess the right kidney in a rat model of diabetes: (a) T2* weighted image used to show structures of the cortex and medulla and to provide a reference for measuring R2* values; and (b) and (c) R2* and T2* map, respectively; and (d) time signal curve of region of interest (ROI) in the cortex and medulla

five ROIs each in the cortex and outer medulla were chosen, respectively, with each ROI comprising 15–30 pixels. The R2* values (mean ± SDs) for cortex and medulla were then calculated. The outer medulla in the renal medullary region was chosen for measurement because Na⁺-K⁺-ATPases are mainly distributed in this area, which consumes almost half the oxygen of the whole kidney,^{17–19} and renal injury has been confirmed by histopathology to occur more easily in this region.^{9,19} In addition,

the inner medulla is influenced by the structure of the renal sinus in R2* maps, which may cause inaccurate measurements.

24-h urinary albumin excretion and blood biochemical examinations

Before BOLD-MRI, rats from the randomly chosen DM group were placed in metabolic cages for 24 h to collect 24-h urine samples. The urine albumin concentration was determined using a Beckman Coulter

IMAGE® 800 Immunochemistry system and associated reagents (Beckman Coulter, Brea, CA, USA) according to the manufacturer's instructions, and then multiplied by 24 h urine volume to get 24 h urinary albumin excretion. Blood creatinine and urea nitrogen were tested from tail vein blood samples using a Beckman Coulter AU5800 Clinical Chemistry System (Beckman Coulter) according to the manufacturer's instructions, and this group was euthanized for histopathological examination, as previously stated.

Histopathological analysis

Rat kidneys were perfused via the abdominal aorta with 1.25 % phosphate buffered glutaraldehyde, pH 7.4, at a constant pressure (100 mmHg). The fixed rat kidney fragments were then cut into 3–4 μm sections and stained with haematoxylin and eosin, and periodic acid-Schiff. The glomerulosclerosis index, stereology of mesangial volume density and capillary surface density were estimated at day 7, 21, 35, 56 and 70, respectively. The glomerulosclerosis index was obtained by measuring the frequency of sclerosis in 100 glomeruli from each animal, as reported previously,²⁰ and the mean \pm SD was calculated. Scores ranged from 0 to 4, depending on the extent of sclerosis: 0, normal glomerulus; 1+, $\leq 25\%$ sclerosis; 2+, $> 25\%$ to $\leq 50\%$ sclerosis; 3+, $> 50\%$ to $\leq 75\%$ sclerosis; and 4+, $> 75\%$ glomerulosclerosis. The glomerulosclerosis index score for every animal was the sum of individual glomerular scores multiplied by the percent of glomeruli with that same score. Stereology of mesangial volume density and capillary surface density were estimated using a test grid (M42) as described previously.²¹ Electron micrographs of each glomeruli were analysed at a magnification of $\times 10\,500$. The capillary surface density (S_v) was estimated by counting the number of intersections

between the capillary surface and the test line (I_L), where $S_v = 2 \times I_L$. The reference volume was determined by counting the test points that hit the glomeruli (P_T). The volume density of this structure was estimated by counting the number of points that hit the mesangium (P_P), where $V_v = P_P/P_T$.

Statistical analyses

Data are presented as mean \pm SD. Statistical analyses were performed using IBM SPSS Statistics package, version 19.0 (IBM, Chicago, IL, USA). Comparison of R^2 values and histopathological results at each time-point between the DM and NC groups were performed using Student's *t*-test. A *P* value < 0.05 was considered statistically significant.

Results

Experimental model characteristics

A total of 65 rats were successfully induced by STZ in the DM group, however, three rats from the DM group died during the study, one died of anaesthesia and two died of diabetic ketoacidosis. Thus, 62 rats in the DM group (12 or 13 rats in each of the five subgroups), and 10 rats in the NC group were included in the final analyses (Table 1). Rats in the DM group displayed polydipsia, polyphagia, polyuria, dispirited spirit, weight loss and poor fur colour. Some rats appeared with genital infection and gradually developed cataract after 6 weeks. Body weights of rats in the DM group were lower than in the NC group after day 3 ($P < 0.001$), and continued to decrease gradually. Kidney size (evaluated by measuring the largest diameter point of the right kidney) increased gradually following day 7, but was not significantly different from the NC group ($P > 0.05$). There were no statistically significant differences

Table 1. Physiological changes in a streptozotocin-induced rat model of diabetes (n = 62) and in normal rat controls (n = 10)

Study group	Study time-point												
	Baseline	Day 3	Day 7	Day 14	Day 21	Day 28	Day 35	Day 42	Day 49	Day 56	Day 63	Day 70	
NC (n=10)	(n=10)	(n=10)	(n=10)	(n=10)	(n=10)	(n=10)	(n=10)	(n=10)	(n=10)	(n=10)	(n=10)	(n=10)	
Body weight, g	217.6 ± 6.12	239.8 ± 6.06	249.3 ± 6.74	279.7 ± 9.24	331.5 ± 9.46	354.1 ± 11.62	368.6 ± 11.22	377.9 ± 12.06	409.2 ± 16.72	421.5 ± 18.62	431.3 ± 24.59	444.1 ± 20.15	
Kidney diameter, cm	22.3 ± 2.13	22.4 ± 1.23	22.5 ± 1.56	23.3 ± 2.36	23.3 ± 3.98	23.3 ± 3.36	24.3 ± 2.87	24.5 ± 2.68	24.5 ± 1.5	25.0 ± 3.23	25.3 ± 2.13	25.4 ± 3.23	
Blood glucose, mmol/l	4.6 ± 1.07	4.7 ± 2.36	4.7 ± 2.34	4.9 ± 2.12	4.9 ± 1.09	4.7 ± 2.13	4.8 ± 2.09	4.8 ± 1.56	4.7 ± 2.36	4.7 ± 1.79	4.6 ± 2.03	4.6 ± 2.45	
DM (n=62) ^a	(n=12)	(n=12)	(n=12)	(n=12)	(n=12)	(n=12)	(n=12)	(n=12)	(n=12)	(n=13)	(n=13)	(n=13)	
Body weight, g	219.7 ± 4.42	214.3 ± 4.46**	216.8 ± 6.07**	212.2 ± 10.68**	207.3 ± 15.21**	197.5 ± 20.77**	192.6 ± 10.96**	189.4 ± 15.28**	187.7 ± 19.04**	195.4 ± 14.31**	197.3 ± 10.28**	197.9 ± 11.13**	
Kidney diameter, cm	22.5 ± 2.32	23.2 ± 1.56	23.3 ± 2.23	24.2 ± 3.21	24.1 ± 2.33	24.5 ± 3.26	24.8 ± 1.89	25.0 ± 2.56	25.7 ± 2.89	25.6 ± 3.21	26.1 ± 1.78	26.3 ± 1.56	
Blood glucose, mmol/l	4.7 ± 1.09	17.32 ± 2.36**	20.3 ± 3.56**	28.6 ± 2.69**	≥33.3**	≥33.3**	≥33.3**	≥33.3**	≥33.3**	≥33.3**	≥33.3**	≥33.3	

Data presented as mean ± SD.

NC, normal controls; DM, diabetes mellitus group.

^aDM subgroups were randomly selected for testing at each time-point.

**P < 0.001 or **P < 0.001, compared with controls (Student's t-test).

in blood sugar levels between the control and DM groups at baseline, however, blood sugar levels ≥ 33.3 mmol/l were reached in the DM group by day 21 (Table 1).

Urinary albumin excretion, blood biochemistry and pathology findings

Urinary albumin excretion in the DM group increased gradually, and was significantly higher than that of the NC group from day 7 (DM, 1.20 ± 0.08 mg/24 h; NC, 1.11 ± 0.17 mg/24 h; $P < 0.01$; Table 2). Serum creatinine and blood urea nitrogen values increased in the DM group over time (serum creatinine levels increased from $12 \mu\text{mol/l}$ at day 28 to $38 \mu\text{mol/l}$ at day 70, and blood urea nitrogen levels increased from 7.7 mmol/l at day 28 to 16.6 mmol/l at day 70). Both parameters were higher in the DM than NC group (creatinine range, $10\text{--}11 \mu\text{mol/l}$ and blood urea nitrogen range, $6\text{--}7$ mmol/l).

The glomerulosclerosis index was higher in the DM group than the NC group from day 56 ($P < 0.01$). Mesangial volume density and capillary surface density was increased in the DM group compared with the NC group ($P < 0.01$ on day 70, and $P < 0.01$ from day 35, respectively; Table 3).

BOLD-MRI results

Renal $R2^*$ values in the DM group rats were significantly higher than in the NC group rats at all time-points following induction of diabetes ($P < 0.01$; Table 4 and Table 5). $CR2^*$ and $MR2^*$ values in the DM group were $28.30 \pm 0.59 \text{ s}^{-1}$ and $31.87 \pm 0.74 \text{ s}^{-1}$ at baseline, then increased gradually to peak at day 35 ($CR2^*$, $33.95 \pm 0.34 \text{ s}^{-1}$, $MR2^*$, $43.79 \pm 1.46 \text{ s}^{-1}$). Following day 35, values gradually decreased to $33.17 \pm 0.69 \text{ s}^{-1}$ ($CR2^*$) and $41.61 \pm 0.95 \text{ s}^{-1}$ ($MR2^*$) at day 70 (Table 4 and Table 5, and Figure 2). Baseline MCR in the DM group was 1.12,

Table 2. Urinary albumin excretion over time in a streptozotocin-induced rat model of diabetes ($n = 62$) and normal controls ($n = 10$)

Study group	Urinary albumin excretion (mg/24 h)													
	Baseline	Day 3	Day 7	Day 14	Day 21	Day 28	Day 35	Day 42	Day 49	Day 56	Day 63	Day 70		
NC ($n = 10$)	1.1 ± 0.1 ($n = 12$)	1.1 ± 0.1 ($n = 12$)	1.1 ± 0.2 ($n = 12$)	1.2 ± 0.1 ($n = 12$)	1.2 ± 0.2 ($n = 12$)	1.2 ± 0.2 ($n = 12$)	1.2 ± 0.1 ($n = 12$)	1.3 ± 0.2 ($n = 12$)	1.2 ± 0.1 ($n = 12$)	1.2 ± 0.2 ($n = 13$)	1.3 ± 0.1 ($n = 13$)	1.3 ± 0.1 ($n = 13$)		
DM ($n = 62$) ^a	1.0 ± 0.1 ($n = 12$)	1.1 ± 0.1 ($n = 12$)	$1.2 \pm 0.1^*$ ($n = 12$)	$1.7 \pm 0.2^*$ ($n = 12$)	$2.3 \pm 0.2^*$ ($n = 12$)	$2.5 \pm 0.3^*$ ($n = 12$)	$3.3 \pm 0.8^{**}$ ($n = 12$)	$3.5 \pm 1.4^{**}$ ($n = 12$)	$3.8 \pm 0.6^{**}$ ($n = 12$)	$4.9 \pm 0.5^{**}$ ($n = 13$)	$5.0 \pm 0.5^{**}$ ($n = 13$)	$6.0 \pm 0.7^{**}$ ($n = 13$)		

Data presented as mean \pm SD.

NC, normal controls; DM, diabetes mellitus group.

^aDM subgroups were randomly selected for testing at each time-point.

* $P < 0.01$ or ** $P < 0.001$, compared with controls (Student's *t*-test).

Table 3. Histopathological examination of the right kidney in a streptozotocin-induced rat model of diabetes ($n = 62$) and normal controls ($n = 10$)

Study group/ time-point	Glomerulosclerosis index (%)	Mesangial volume density (%)	Capillary surface density (mm^2/mm^3)
NC, day 70 ($n = 10$)	1.36 ± 0.3	11 ± 1.2	0.29 ± 0.02
DM, day 7 ($n = 12$)	1.42 ± 0.2	12 ± 0.25	0.3 ± 0.1
DM, day 21 ($n = 12$)	1.48 ± 0.4	13.2 ± 0.3	0.32 ± 0.4
DM, day 35 ($n = 12$)	2.1 ± 0.5	13.9 ± 0.3	$0.38 \pm 0.06^*$
DM, day 56 ($n = 13$)	$3.7 \pm 0.7^*$	13.6 ± 0.26	$0.40 \pm 0.7^*$
DM, day 70 ($n = 13$)	$5.5 \pm 0.5^*$	$14.5 \pm 1.0^*$	$0.42 \pm 0.11^*$

Data presented as mean \pm SD.

NC, normal controls; DM, diabetes mellitus group.

* $P < 0.01$ compared with controls (Student's *t*-test).

which rose to 1.32 at day 42, then dropped down to 1.25 at day 70 (Figure 2).

Discussion

According to published diabetic nephropathy diagnostic criteria,²² data from the present study regarding urinary albumin excretion and pathological changes indicate that the present diabetic rats were in nephropathy stage I within 7 days, nephropathy stage II within 7–35 days, and nephropathy stage III within days 35–70 days. The present BOLD-MRI results showed that CR2* and MR2* values within the experimental period in the DM group were increased compared with controls, suggesting decreased oxygenation in both the renal cortex and medulla at different time-points in the presence of diabetes, consistent with previous reports.^{9–11,23} Hypoxic changes in diabetic kidneys may be due to the hyperfiltration phenomenon seen early after induction of diabetes, whereby the high filtration and high metabolic rates activate renal tubular reabsorption and Na⁺/K⁺-ATPase activity, resulting in increased oxygen consumption.^{9,24,25} A previous study documented that renal tubules in rats with diabetes consumed >40% more oxygen than those in non-diabetic rats.⁹ In addition, an

evaluation of the influence of STZ-induced diabetes on renal pO₂ and blood flow, using invasive microprobes and BOLD-MRI,¹⁰ suggested that hypoxic changes are not dependent on blood flow until 28 days after induction of diabetes, and these changes can be detected as early as 2 days in rat kidneys by BOLD-MRI. The present results showed that microalbuminuria differed between normal controls and a rat model of diabetes from day 7 following induction of diabetes, but cortex and medulla R2* values were significantly higher than controls from day 3, and showed an increasing trend, in the DM group. These results may indicate that BOLD-MRI can detect renal oxygen changes earlier and more sensitively than microalbuminuria.

The present study continued for up to 70 days, and the remaining diabetic rats developed hyperglycaemia, eye cataracts and raised urinary microproteins, suggesting progressive kidney damage. Hypoxia peaked on day 35, and after this time, kidney R2* values in diabetic rats decreased. The present results showed a rising then falling trend in CR2* and MR2* values during diabetic renal injury. That is, when the glomerulosclerosis index and capillary surface density increased significantly from day 35, the diabetic rats in

Table 4. Changes in CR2* values over time, measured using blood oxygenation level dependent-magnetic resonance imaging, in a streptozotocin-induced rat model of diabetes (n = 62) and normal controls (n = 10)

Time-point												
Study Group	Baseline	Day 3	Day 7	Day 14	Day 21	Day 28	Day 35	Day 42	Day 49	Day 56	Day 63	Day 70
CR2* values (s ⁻¹)												
NC	28.4 ± 0.7 (n = 12)	28.5 ± 0.8 (n = 12)	28.6 ± 1.2 (n = 12)	28.4 ± 0.5 (n = 12)	28.1 ± 0.9 (n = 12)	28.2 ± 0.7 (n = 12)	28.6 ± 0.7 (n = 12)	28.7 ± 0.5 (n = 12)	28.1 ± 1.1 (n = 12)	28.2 ± 0.7 (n = 13)	28.3 ± 0.6 (n = 13)	28.4 ± 0.6 (n = 13)
DM ^a	28.3 ± 0.6	31.1 ± 0.5**	31.4 ± 0.6**	32.5 ± 0.7**	33.0 ± 0.6**	33.6 ± 0.3**	34.0 ± 0.3**	33.1 ± 0.7**	32.6 ± 0.4**	32.6 ± 0.6**	32.6 ± 0.6**	33.2 ± 0.7**

Data presented as mean ± SD.

NC, normal controls; DM, diabetes mellitus group.

^aDM subgroups were randomly selected for testing at each time-point.

**P < 0.001 compared with controls (Student's t-test).

Table 5. Changes in MR2* values over time, measured using blood oxygenation level dependent-magnetic resonance imaging, in a streptozotocin-induced rat model of diabetes (n = 62) and normal controls (n = 10)

Time-point												
Study Group	Baseline	Day 3	Day 7	Day 14	Day 21	Day 28	Day 35	Day 42	Day 49	Day 56	Day 63	Day 70
MR2* values (s ⁻¹)												
NC	31.5 ± 0.9 (n = 12)	32.1 ± 1.3 (n = 12)	31.7 ± 1.5 (n = 12)	31.5 ± 1.2 (n = 12)	31.8 ± 1.6 (n = 12)	30.7 ± 0.7 (n = 12)	31.9 ± 1.4 (n = 12)	31.2 ± 0.9 (n = 12)	31.5 ± 0.6 (n = 12)	30.8 ± 1.2 (n = 13)	31.2 ± 0.9 (n = 13)	31.8 ± 0.9 (n = 13)
DM ^a	31.9 ± 0.7	36.1 ± 0.8**	37.6 ± 0.6**	39.3 ± 0.4**	40.8 ± 1.0**	41.8 ± 0.8**	43.8 ± 1.5**	43.6 ± 1.3**	42.0 ± 1.0**	41.2 ± 0.9**	41.9 ± 0.9**	41.6 ± 1.0**

Data presented as mean ± SD.

NC, normal controls; DM, diabetes mellitus group.

^aDM subgroups were randomly selected for testing at each time-point.

**P < 0.001 compared with controls (Student's t-test).

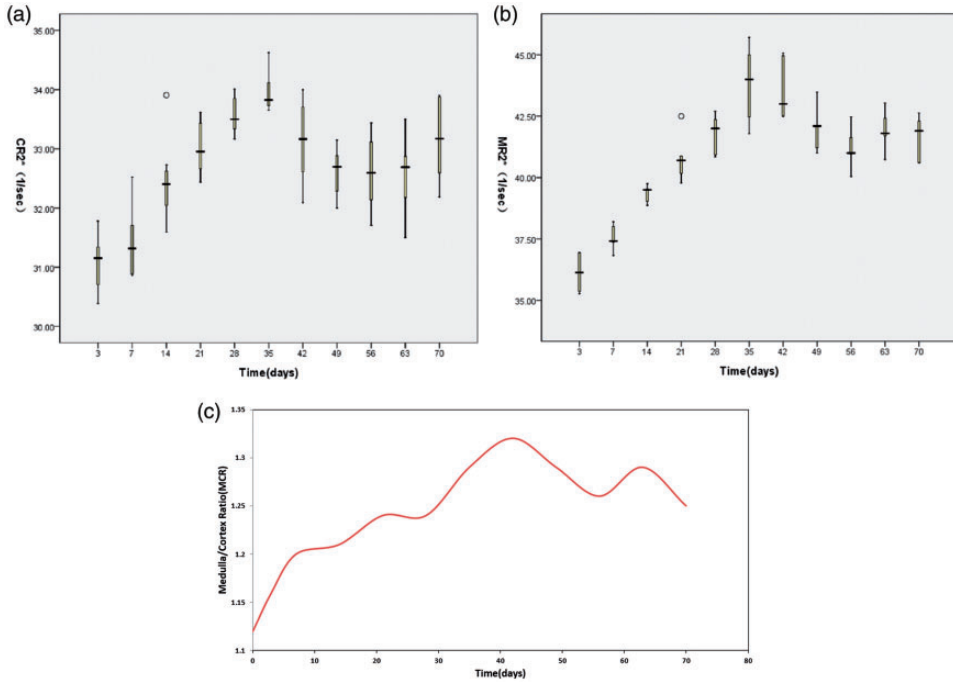


Figure 2. Box-whisker plots showing: (a) Changes in cortex (C)R2* values in a streptozotocin-induced rat model of diabetes mellitus (DM group) over 70 days (s⁻¹); (b) Changes in medulla (M)R2* values in the DM group over 70 days (s⁻¹); and (c) Changes in the medulla to cortex ratio (MCR) in the DM group over 70 days; the heavy black horizontal lines are medians, the extremities of the box are the 25th and 75th percentiles, the error bars represent minimum and maximum outliers, the circles above the day 14 and 21 bars represent extreme outliers

the present study were at nephropathy stage II to stage III. Interestingly, decreasing CR2* and MR2* values suggested that renal hypoxia status was improved during this period, however, this phenomenon was not found in similar published reports, and BOLD-MRI cannot differentiate between changes oxygen supply versus demand.

The mechanism of hypoxia change cannot be explained clearly by the present study, however, an invasive investigation of renal function in diabetic rats in nephropathy stages II and III,¹⁴ demonstrated that glomerular filtration rate (GFR) was always much higher in rats with diabetes

than controls. Also, renal plasma flow was gradually increased and renal vascular resistance reduced accordingly, from stages II to stages III. Thus, the kidney oxygen supply should be increased because of increasing blood flow. This may explain the descending part of the dynamic R2* curve in the present results, which may have been due to haemodynamic changes leading to increased blood supply in the renal cortex and medulla, and subsequently, improved renal oxygenation.

In support of the present results, a similar BOLD-MRI R2* pattern has been shown in patients with type 2 diabetes,¹¹

and hypoxia was documented to be predominantly caused by hyper metabolism during the early clinical stage of diabetic nephropathy, with oxygen consumption decreasing gradually in later stages, as a result of lower workload. That is, the deterioration of tubular function and lower GFR probably raised pO_2 in the medullary region, although $MR2^*$ in diabetic nephropathy was markedly higher compared with controls.¹¹ The present results are also supported by other studies that investigated rats with renal artery stenosis.^{26,27} For example, after 4 weeks, no renal hypoxia was detected by BOLD-MRI in the rat kidney downstream of a renal artery stenosis,²⁶ and in another study, remnant kidneys had 73% increased oxygen tensions (measured using needle electrodes) in both the cortex and outer medulla for 6–8 weeks following ligation of branches of the renal artery,²⁷ suggested to be due to higher oxygen tensions caused by a decrease in filtration fraction, or due to a possible adaptive mechanism. In addition to the above explanations, other factors may be involved in reduced oxygen consumption, such as renal tubule cells maintaining concentration and dilution function of the urine, and elevated levels of oxidative stress and inflammatory responses of the renal tissues causing dysfunction of renal tubule cells.^{22,28,29} Combinations of all these factors have been reported to be associated with changes in BOLD-MRI signals compared with controls.

The $CR2^*$ and $MR2^*$ value can be influenced by magnetic field inhomogeneity, coil position and the physiological condition of subject,^{8,29,30} thus, the medulla to cortex $R2^*$ ratio (MCR) was also calculated in the present study, to decrease the effect of these factors. In the present study, dynamic changes in the diabetic MCR resembled a downward parabola. This complicated MCR reverse change is similar to that seen in patients with diabetic nephropathy

from stage III into stage IV,¹¹ and is important for patients, as it means the disease deteriorates from early to later stages. Mesangial proliferation is significant and nodular sclerosis appears pathologically at this point, however, patients take a long time to develop from stage I to stage IV and are more difficult to diagnose in the early stages, due to absence of symptoms.³¹ Patients may, therefore, lose treatment opportunities to improve renal oxygenation. BOLD-MRI can detect oxygenation changes earlier than pathological changes, so the reversion of MCR in the present results may indicate that the kidney hypoxia was a result of increasing oxygen consumption during the early clinical stage of diabetic nephropathy leading to haemodynamic and architectural modification. Thus, the reversion of MCR may indicate kidney change from functional compensatory changes to organic lesions. Observation of MCR may, therefore, have great significance for physicians in prevention and control of diabetic renal injury.

The results of the present study may be limited by several factors. First, the sample number in the experimental group was relatively small at the later stages, due to the limited number of remaining rats. Secondly, the change in renal oxygenation levels in diabetic rats treated with insulin, particularly in stage II diabetic rats, was not investigated, but would be the present authors' future direction of research. Thirdly, changes in serum glucose and glycosylated haemoglobin (HbA_{1c}) levels were not measured at time-points during which $R2^*$ values were measured. HbA_{1c} is the standard measure of glycaemic control, and the HbA_{1c} value can be used to estimate average glucose.³² The impact of HbA_{1c} on the $R2^*$ value has been recognised, and the most obvious effect of hyperglycaemia in the human body is on brain tissue. Acute changes in glycaemia can lead to hemiparesis and confusion.³³ A study to determine

the effect of plasma glucose on BOLD-MRI $R2^*$ values in six healthy humans,³⁴ found that severe acute hyperglycaemia did not appear to substantially effect BOLD-MRI values. In addition, there are currently no published reports regarding the effects of hyperglycaemia and HbA_{1C} on $R2^*$ values in the kidneys of diabetic rats. Hyperglycaemia also affects volume and tissue water content in the kidney. In the present study, the rats had free access to water and food, and differences in renal $R2^*$ values between diabetic rats and normal controls has been suggested to be caused by water diuresis (however, no statistical significance was shown).⁹ The present study did not control for diuresis, so the effect may not be excluded.

In conclusion, the dynamic changes in $R2^*$ values in a rat model of diabetes showed a rising then falling trend in early diabetic renal injury. At first, $R2^*$ values appear to reflect renal hypoxia, and are more sensitive in detecting early renal changes compared with microalbuminuria. Then, renal oxygenation appears to be elevated and renal hypoxia is improved. The reversal of MCR seen in the present study may indicate renal injury from increased oxygen consumption to increased blood supply, and might be a reversible transition stage for diabetes, and thus, may be expected to become a sensitive indicator for evaluating the degree of renal injury.

Declaration of conflicting interests

The authors declare that there is no conflict of interest.

Funding

This study was supported by grants from the Natural Science Foundation of Zhejiang Province (Grant No. 2015C33138), and from the Science and Technology Department of Public Welfare Projects of Zhejiang Province (Grant No. LZ16H180001).

References

1. Wang B, Lin L, Ni Q, et al. Chinese medicine for treating diabetic nephropathy. *Chin J Integr Med* 2011; 17: 794–800.
2. Miyata T, Takizawa S and van Ypersele de Strihou C. Hypoxia.1. Intracellular sensors for oxygen and oxidative stress: novel therapeutic targets. *Am J Physiol Cell Physiol* 2011; 300: 226–231.
3. Sahin N, Solak A, Genc B, et al. Brain diffusion changes in unilateral carotid artery stenosis with non-shunt endarterectomy: Correlation with white matter lesions. *Clin Neurol Neurosurg* 2015; 133: 24–29.
4. Winfield JM, deSouza NM, Priest AN, et al. Modelling DW-MRI data from primary and metastatic ovarian tumours. *Eur Radiol* 2015; 25: 2033–2040.
5. Prasad PV, Edelman RR and Epstein FH. Noninvasive evaluation of intrarenal oxygenation with BOLD MRI. *Circulation* 1996; 94: 3271–3275.
6. Thoeny HC, Zumstein D, Simon-Zoula S, et al. Functional evaluation of transplanted kidneys with diffusion-weighted and BOLD MR imaging: initial experience. *Radiology* 2006; 241: 812–821.
7. Ogawa S, Lee TM, Kay AR, et al. Brain magnetic resonance imaging with contrast dependent on blood oxygenation. *Proc Natl Acad Sci USA* 1990; 87: 9868–9872.
8. Pedersen M, Dissing TH, Mørkenborg J, et al. Validation of quantitative BOLD MRI measurements in kidney: application to unilateral ureteral obstruction. *Kidney Int* 2005; 67: 2305–2312.
9. Ries M, Basseau F, Tyndal B, et al. Renal diffusion and BOLD MRI in experimental diabetic nephropathy. *J Magn Reson Imaging* 2003; 17: 104–113.
10. Dos Santos EA, Li LP, Ji L, et al. Early changes with diabetes in renal medullary hemodynamics as evaluated by fiberoptic probes and BOLD magnetic resonance imaging. *Invest Radiol* 2007; 42: 157–162.
11. Yin WJ, Liu F, Li XM, et al. Noninvasive evaluation of renal oxygenation in diabetic nephropathy by BOLD-MRI. *Eur J Radiol* 2012; 81: 1426–1431.

12. Wang ZJ, Kumar R, Banerjee S, et al. Blood oxygen level-dependent (BOLD) MRI of diabetic nephropathy: preliminary experience. *J Magn Reson Imaging* 2011; 33: 655–660.
13. Hueper K, Hartung D, Gutberlet M, et al. Magnetic resonance diffusion tensor imaging for evaluation of histopathological changes in a rat model of diabetic nephropathy. *Invest Radiol* 2012; 47: 430–437.
14. Lopes GS, Lemos CCS, Mandarim-De-Lacerda CA, et al. Effect of unilateral nephrectomy on renal function of diabetic rats. *Histol Histopathol* 2004; 19: 1085–1088.
15. Szkudelski T. The mechanism of alloxan and streptozotocin action in B cells of the rat pancreas. *Physiol Res* 2001; 50: 537–546.
16. Alhaider AA, Korashy HM, Sayed-Ahmed MM, et al. Metformin attenuates streptozotocin-induced diabetic nephropathy in rats through modulation of oxidative stress genes expression. *Chem Biol Interact* 2011; 192: 233–242.
17. Farman N, Corthesy-Theulaz I, Bonvalet JP, et al. Localization of alpha-isoforms of Na(+)-K(+)-ATPase in rat kidney by in situ hybridization. *Am J Physiol* 1991; 260: 468–474.
18. Chamberlin ME, LeFurgey A and Mandel LJ. Suspension of medullary thick ascending limb tubules from the rabbit kidney. *Am J Physiol* 1984; 247:F955–964.
19. Brezis M, Rosen S, Silva P, et al. Selective anoxic injury to thick ascending limb: an anginal syndrome of the renal medulla? *Adv Exp Med Biol* 1984; 180: 239–249.
20. Raij L, Azar S and Keane W. Mesangial immune injury, hypertension and progressive glomerular damage in Dahl rats. *Kidney Int* 1984; 26, 137–143.
21. Nyengaard JR. Stereologic methods and their application in kidney research. *J Am Soc Nephrol* 1999; 10, 1100–1123.
22. Mogensen CE, Schmitz A and Christensen CK. Comparative renal pathophysiology relevant to IDDM and NIDDM patients. *Diabetes Metab Rev* 1988; 4: 453–483.
23. Prasad P, Li LP, Halter S, et al. Evaluation of renal hypoxia in diabetic mice by BOLD MRI. *Invest Radiol* 2010; 45: 819–822.
24. Baines A and Ho P. Glucose stimulates O₂ consumption, NOS, and Na/H exchange in diabetic rat proximal tubules. *Am J Physiol Renal Physiol* 2002; 283: F286–F293.
25. Palm F, Fasching A, Hansell P, et al. Nitric oxide originating from NOS1 controls oxygen utilization and electrolyte transport efficiency in the diabetic kidney. *Am J Physiol Renal Physiol* 2010; 298: F416–F420.
26. Rognant N, Guebre-Egziabher F, Bacchetta J, et al. Evolution of renal oxygen content measured by BOLD MRI downstream a chronic renal artery stenosis. *Nephrol Dial Transplant* 2011; 26: 1205–1210.
27. Priyadarshi A, Periyasamy S, Burke TJ, et al. Effects of reduction of renal mass on renal oxygen tension and erythropoietin production in the rat. *Kidney Int* 2002; 61: 542–546.
28. Yan SF, Ramasamy R and Schmidt AM. Receptor for AGE (RAGE) and its ligands—cast into leading roles in diabetes and the inflammatory response. *J Mol Med (Berl)* 2009; 87: 235–247.
29. Ehlermann P, Eggers K, Bierhaus A, et al. Increased proinflammatory endothelial response to S100A8/A9 after preactivation through advanced glycation end products. *Cardiovasc Diabetol* 2006; 5: 6.
30. Eckardt KU, Bernhardt WM, Weidemann A, et al. Role of hypoxia in the pathogenesis of renal disease. *Kidney Int Suppl* 2005; 99: S46–S51.
31. Afroz T, Sagar R, Reddy S, et al. Clinical and histological correlation of diabetic nephropathy. *Saudi J Kidney Dis Transpl* 2017; 28: 836–841.
32. Behan KJ, Mbizo J, Johnston MA, et al. Does race alter the relationship between HbA1c and glucose in type 2 diabetes? *Clin Lab Sci* 2014; 27: 89–96.
33. Arieff A and Carroll H. Nonketotic hyperosmolar coma with hyperglycemia: clinical features, pathophysiology, renal function, acid-base balance, plasma-cerebrospinal fluid equilibria and the effects of therapy in 37 cases. *Medicine* 1972; 51: 73–94.
34. Gruetter R, Uğurbil K and Seaquist ER. Effect of acute hyperglycemia on visual cortical activation as measured by functional MRI. *J Neurosci Res* 2000; 62: 279–285.